11

# An iterative method for solving the problem of diffraction on a nonlinear dielectric lattice in strong electromagnetic fields


A.M. Lerer, I.N. Ivanova, V.I. Kravchenko

Southern Federal University,
344090 Rostov-on-Don, Russia
e-mail: lerer@sfedu.ru

Received January 15, 2025
Revised January 15, 2025
Accepted January 15, 2025

Three problems of nonlinear electrodynamics have been solved. An analytical solution of boundary value problems on the reflection of an electromagnetic wave from a dielectric layer coated with nonlinear graphene and from a nonlinear dielectric layer is presented. A method for solving a nonlinear integro-differential equation (IDE) of the second kind for diffraction problems on a nonlinear dielectric body is proposed. It is shown that an IDE can be transformed to an IDE with a linear integral term and a nonlinear free term. This significantly increases the speed of calculations. An iterative method has been implemented to solve the transformed IDE.

**Keywords:** nonlinear dielectric, graphene, reflection, diffraction, integro-differential equation, Galerkin method, perturbation method.

DOI: 10.61011/TP.2025.05.61137.2-25

## Introduction

Non-linear meta-surfaces that involve the use of both, conventional dielectrics and plasmon materials (metals in the optical band, graphene) and their combinations, are widespread in todays' photonics — sensors, visualization, optical multiplexing, generation of upper harmonics, terahertz emission, entangled photons [1–12]. The main advantages of meta-surfaces are their small sizes, ability to control the wave front by manipulating the linear phase of transmitted or reflected light, and the presence of resonance elements. To increase the level of harmonic generation and mixing, it is natural to use resonances, including plasmon — polariton resonances, resonance of localized plasmons. Although, as stated in [13,14], graphene has greater nonlinearity than dielectrics, graphene meta-surfaces have greater losses compared to dielectric ones. Therefore, dielectric resonant meta-surfaces can operate at high power.

The purpose of this paper is to show the possibility of numerically analytical solutions of reflection and diffraction problems on nonlinear meta-surfaces in strong electromagnetic fields, and to estimate the error of the perturbation method.

Objects under study: 1) nonlinear graphene layer; 2) diffraction grating formed by nonlinear dielectric layers; 3) nonlinear dielectric layer for testing the volumetric integro-differential equation (IDE) method.

## 1. Reflection of electromagnetic wave from a graphene layer lying on a dielectric layer

It has been theoretically and experimentally established that graphene has an extremely strong third-order nonlinearity compared to widely used dielectrics. This is due to the appearance of a large number of papers (mostly theoretical) on the development of nonlinear photonic devices [15].

The simplest way to solve a nonlinear problem is the perturbation method — to use the electrical field strength obtained from solving a linear problem. However, it is possible to obtain an analytical solution for the simple problem of reflecting a planar electromagnetic wave from a graphene layer [16]. The task set in this section — to ensure progress of the study [16].

Coordinate system — $z$ axis is perpendicular to the plane-parallel dielectric layer $h$ thick and dielectric permittivity of $\varepsilon_1$. Planar electromagnetic wave has an incidence angle of $\theta$ from $z = -\infty$. Incidence plane $x = 0$. Graphene layer is located at the bottom face of the layer with a coordinate $z = 0$. At $z \geq h$ the substrate has dielectric permittivity $\varepsilon_2$. Wave polarization along $x$ axis— $\mathbf{E} = E\mathbf{e}_x$. The orthogonal polarization solution is similar. Only boundary conditions (BC) at the interfaces of dielectric layers change.

BC:

1) continuity $E$ at all boundaries, including at infinitely thin graphene layer;

2) continuity of the component of magnetic field $H_y$ at $z = h$;

3) impedance BC on graphene $j(y) = \sigma E(y, 0)$, where $j(y)$, $\sigma$-conductivity, — $\sigma(E_g) = \sigma_1 + \sigma_3|E_g|^2$, $E_g$ — strength of electrical field on graphene where $\sigma_1$ — linear conductivity from Kubo formula [17], $\sigma_3$ — non-linear conductivity of graphene third order. For THz to optical band frequencies, the nonlinear conductivity of graphene of the third order is determined by a formula based on quantum theory [18,19]. Various formulae for calculating the nonlinear conductivity of graphene compared are given in the review [20]. The following formula was used in the

present work.

$$\sigma_3 = -i\frac{3}{32}\frac{e^4 v_F^2}{\omega^3\hbar^2\mu_c},$$

where $e$ — electron charge, $\mu_c$ — chemical potential (Fermi level), $v_F = 10^6$ m/s — Fermi velocity, $\omega$ — frequency of incident wave, $\hbar$ — reduced Planck's constant. This formula is applicable with the quant energy of $\hbar\omega \ll 2\mu_c$.

It is not difficult to obtain a solution of Helmholtz equation for a field in a dielectric satisfying the first BC:

$$E(y,z) = E_0 \times \begin{cases} \exp\left[i(-k_{z,1}z + k_{y,1}y)\right]\exp(i\omega t) + \sum\limits_{j=1,3}(A_j - \delta_{j,1}) \\ \quad \times \exp\left[i(k_{z,j}z + k_{y,j}y)\right]\exp(ij\omega t),\ z \le 0 \\ \sum\limits_{j=1,3}\frac{1}{\sin\gamma_{1,j}h}\left[A_j \sin\gamma_{1,j}(h-z) + T_j\sin\gamma_{1,j}z\right] \\ \quad \times \exp(ik_{y,j}y)\exp(ij\omega t),\ 0 \le z \le h \\ \sum\limits_{j=1,3} T_j \exp\left[-i\gamma_{2,j}(z-h) + ik_{y,j}y\right]\exp(ij\omega t), \\ \quad z \ge h \end{cases},$$

where $E_0$ — amplitude of incident wave,

$$k_{y,3} = k_{y,1} = k_1\sin\theta, \quad k_{z,j} = \sqrt{k_j^2 - k_{y,1}^2},$$

$$\gamma_{\{{1 \atop 2}\},j} = \sqrt{k_j^2\varepsilon_{\{{1 \atop 2}\}} - k_{y,1}^2}, \quad k_1,\ k_3 = 3k_1$$

— wavenumbers of the first and third frequency harmonics.

Having satisfied the second boundary condition, we express the unknown coefficients $A_j$ in terms of the desired transmission ratio $T_j$:

$$A_j = U_j T_J, \quad U_j = \cos\gamma_{1,j}h + \frac{i\gamma_{2,j}}{\overline{\gamma}_{1,j}}\sin\gamma_{1,j}h.$$

Finally, having satisfied the third BC we get

$$-\frac{1}{Z_0}\left\{\frac{k_{z,1}}{k_1} - \sum_{j=1,3}(T_jU_j - \delta_{j,1})\frac{k_{z,j}}{k_j}\exp(ij\omega t) - i\sum_{j=1,3}T_jV_j\exp(ij\omega t)\right\} = \sigma\left[\exp(i\omega t) + \sum_{j=1,3}(T_jU_j - \delta_{j,1})\exp(ij\omega t)\right], \tag{1}$$

where $V_j = \frac{\gamma_{1,j}}{k_j}\left[-\left(\frac{i\gamma_{2,j}}{\gamma_{1,j}}\right)\cos\gamma_{1,j}h + \sin\gamma_{1,j}h\right]$.

From BC for the fundamental harmonic, after elementary transformations, we obtain

$$T_1\left[U_1\left(1 - \sigma\frac{k_1}{k_{z,1}}\right) + iV_1\frac{k_1}{k_{z,1}}\right], \tag{2}$$

at

$$\sigma(|T_1|) = \sigma_1 + \sigma_3\frac{3}{4}\left[E_0^2\left[|U_1||T_1|\right]^2\right]. \tag{3}$$

It follows from (1) that

$$|T_1|\left[U_1\left(1 - \sigma(|T_1|)\frac{k_1}{k_{z,1}}\right) + iV_1\frac{k_1}{k_{z,1}}\right] = 2. \tag{4}$$

Equation (4) with conductivity (3) — transcendental equation relative to the unknown $|T_1|$. First, we find numerical solution, after that - $\sigma(|T_1|)$ from (3), and then from (2) we find complex transmission ratio $T_1$ and reflectance $R_1 = U_1T_1 - 1$. If we know $T_1$, from (1) we may find the coefficients for the third harmonic $T_3, R_3$.

## 2. Reflection from the non-linear layer

The structure is similar to the one described above, but without graphene, while in a layer with a thickness of $h$ there is a dielectric with quadratic nonlinearity $\varepsilon(y) = \varepsilon_{lin} + \alpha|E(x)|^2$. In solution the non-linear layer is dissected in $N$-layers. We assume that within each layer, the dielectric constant is constant, depending on the field strength in the center of the layer.

The task set in this section — to ensure progress of the study [21,22].

We introduce the functions: a) $U(y,z,t) = E_x(y,z,t)$ for $s$-polarization of the incident plane wave with cyclic frequency $\omega_1$; b) $U(y,z,t) = H_x(y,z,t)$ for $p$-polarization of the incident plane wave

$$U^{(\exp)}(y,z,t) = U_0\exp[i(-k_yy - k_zz + \omega_1 t)].$$

We'll be limited only by two frequency harmonics. The solution is represented as:

$$U(y,z,t) = [V_1(z)\cos(\omega_1 t) + V_3(z)\cos(\omega_3 t)]\exp(-ik_yz).$$

We assume that $|V_3(z)| \ll |V_1(z)|$.

In this case, Helmholtz equation in the nonlinear layer will take the form

$$\sum_{j=1,3}\left[\frac{d^2V_j}{dz^2} + V_j\left(\kappa_j^2 + k_j^2\alpha|V_1|^2\cos^2(\omega_1 t)\right)\cos(\omega_j t)\right], \tag{5}$$

where $\kappa_j^2 = k_j^2\varepsilon_l - k_x^2$, $k_j$ — wavenumber at cyclic frequency $\omega_j$. Let's write it using harmonics:

$$\frac{d^2V_1}{dz^2} + \gamma_1^2V_1 = 0, \quad \gamma_1^2 = \kappa_1^2 + k_1^2\alpha\frac{3}{4}|V_1|^2, \tag{6}$$

$$\frac{d^2V_3}{dz^2} + \gamma_3^2V_3 + k_1^2\beta V_1 = 0,$$

$$\gamma_3^2 = \kappa_3^2 + k_3^2\alpha\frac{1}{2}|V_1|^2, \quad \beta = \frac{1}{4}\alpha|V_1|^2. \tag{7}$$

The solution of (6) is represented as:

$$V_1z = U_0\begin{cases}[\exp(-ik_zz) + R_1\exp(ik_zz)],\ z \le 0 \\ T_1U_+(z,|T_1|),\ z \ge 0,\end{cases},$$

where $R_1, T_1$ are the desired reflection and transmission coefficients of a wave with a frequency o $\omega_1$. At this stage, we consider the function $U_+(z, |T|)$ to be known. Let's assume that $U_+(0, |T|) = 1$ . Let's describe the way to find it below.

We satisfy the conditions of continuity of the tangential components of the electromagnetic field at $z = 0$. In particular, for $s$-polarization, we obtain

$$1 + R_1 = T_1, \quad 1 - R_1 = T_1\eta, \tag{8}$$

where $\eta(|T_1|) = iU'_+(0, |T_1|)/k_z$, prime — derivative with respect to $z$. From (8) we obtain

$$T_1[1 + \eta(|T_1|)] - 2 = 0. \tag{9}$$

We solve numerically the transcendental equation (9) relatively to unknown $|T_1|$ . Then, from (8), we find the coefficients $R_1$ depending on the field amplitude.

The method of successive approximations for the solution (9) at large wave amplitudes is also used. We assume that $E_0^{(p)} = E_0 \frac{p}{P}$. Let's solve (6) in $P$ steps [18]:

$$T^{(p)} = \frac{2}{1 + \eta(T^{(p-1)})}, \quad p = 1, 2 \dots P,$$

where $T^{(p)}$ — solution at $E_0^{(p)}$, $T^{(0)}$ — linear solution.

The resulting algorithm converges quickly in the number of steps $P$. Both methods give the same solution even at large field amplitudes.

Let's consider plotting the function $U_+(z, |T|)$. Let's divide the layer in $N$-layers. The layers have the same thickness $h_n$. We assume that within each layer $\varepsilon_n$ is constant, depending on the field strength in the center of the layer. $N + 1$ layer — semi-finite linear substrate. Let's denote $z_n = \sum\limits_{m=1}^{n} h_n$.

The solution in this case will be written as

$$U_{(z)} = \left\{ \begin{array}{l} \frac{1}{\sin\gamma_n h_n}[A_n \sin\gamma_n(z_n - z) + A_{n+1}\sin\gamma_n(z - z_{n-1})], \\ \quad n = 1, 2 \dots N \\ A_{N+1}\exp[-i\gamma_{N-1}(z - z_n)] \end{array} \right\},$$

$$\gamma_n = \sqrt{k^2\varepsilon_n - k_y^2}.$$

This solution satisfies the condition of continuity at the interface of the layers. From the condition of continuity of normal derivatives, we obtain a recurrent scheme for determining unknowns $A_n = \tilde{A}_n/\tilde{A}_1$:

$$\tilde{A}_n = Q_n^{-1}\left[\tilde{A}_{n+1}(P_n + P_{n+1}) - \tilde{A}_{n+2}Q_{n+1}\right],$$

$$n = N, N-1, \dots, 1, \tilde{A}_{N+2} = 0, \tilde{A}_{N+1} = 1.$$

$$Q_n = \frac{\gamma_n}{\sin\gamma_n h_n}, \quad P_n = \gamma_n \operatorname{ctg}\gamma_n h_n, \quad n = 1, \dots N,$$

$$P_{N+1} = -i\overline{\gamma}_{N+1}.$$

Having defined all $A_n$, let's find the field in the center of the layer

$$E\left(z_n + \frac{h_n}{2}\right) = E_0 T U_+\left(z_n + \frac{h_n}{2}\right) = \frac{E_0 T[A_n + A_{n+1}]}{\left[2\cos\frac{\gamma_n h_n}{2}\right]},$$

and after that the dielectric permittivity $\varepsilon_n = \varepsilon_{lin} + \alpha|E(z_n + h_n/2)|^2$, where $\varepsilon_{lin}$ — linear dielectric permittivity.

The resulting algorithm converges quickly in the number of partitions $N$.

Now let's solve the equation (8) for the third harmonic. All parameters for the first harmonic are determined at the last step of the direct or iterative method.

Again, the non-linear layer is partitioned in $N$-layers.

Solving an inhomogeneous equation (8) we search in the form of two functions

$$V_3 = V_3^{(1)} + V_3^{(2)},$$

where the 1st function — general solution of the homogeneous equation, $\frac{d^2V_3^{(1)}}{dy^2} + \gamma_3^2 V_3^{(1)} = 0$ in all layers; the 2nd function is the solution of the inhomogeneous equation $\frac{d^2V_3^{(2)}}{dy^2} + k_1^2\beta V_1 = 0$ only in the nonlinear layer.

$$V_3^{(1)}(y) = \begin{cases} R_3\exp(i\gamma_{3,0}y), \quad y \le 0; \\ \frac{1}{\sin\gamma_{3,n}h_n}\left[A_{3,n}\sin\gamma_{3,n}(y_n - y)\right. \\ \left. + B_{3,n}\sin\gamma_{3,n}(y - y_{n-1})\right], \quad n = 1, 2 \dots N \\ T_3\exp(-i\gamma_{3,y-1}(y - y_N)), \quad y \ge y_N; \end{cases}$$

$$V_3^{(2)}(y) = \begin{cases} 0, \quad y \le 0; \\ M_n\frac{1}{\sin\gamma_{1,n}h_n}\left[A_{1,n}\sin\gamma_{1,n}(y_n - y)\right. \\ \left. + A_{1,n+1}\sin\gamma_{1,n}(y - y_{n-1})\right], \quad n = 1, 2 \dots N \\ 0, \quad y \ge y_N; \end{cases}$$

$$M_n = \frac{k_1^2\beta}{(\gamma_{1,n})^2}.$$

Let's provide consistency with the boundary conditions. The procedure is quite simple, but quite bulky, so it is not given here. Finally, we'll obtain a system of linear algebraic equations (SLAE) of $2N + 2$ order relative to the unknowns $A_{3,n}, n = 1, \dots N$; $R_3$; $B_{3,n}, n = 1, \dots N$; $T_3$, from which we'll find $R_3, T_3$ — reflectance and transmission coefficients of wave with a frequency of $\omega_3$.

The resulting algorithm converges quickly in the number of partitions $N$ and number of iterations $P$.

## 3. Diffraction on the non-linear dielectric field

The solution of diffraction on a linear diffraction grating by IDE method with isotropic layers is given in [23]. Solving the volumetric integro-differential equation with respect to

$\mathbf{E}(x, y, z)$ — strength of the external electromagnetic field in nonlinear dielectric strips

$$\mathbf{E}(x, y, z) = \mathbf{E}^{ext}(x, y, z) + [\text{grad div} + k^2] \times \int_V G(\overline{x}, \overline{y}, z, z')\tau(|\mathbf{E}(x', y', z')|)\mathbf{E}(x', y', z')dv',$$

$$x, y, z \in V,$$

where $\mathbf{E}^{ext}$ — strength of external electromagnetic field, $\tau(|\mathbf{E}(x', y', z')|) = \varepsilon - \varepsilon^{ext}$, $\varepsilon$, $\varepsilon^{ext}$ — dielectric permittivity of strips and dielectric, $G(\overline{x}, \overline{y}, z, z')$ — Green's function, $\overline{x} = x - x', \overline{y} = y - y'$.

We assume that the dielectric constant is nonlinear

$$\tau(|\mathbf{E}(x', y', z')|) = \varepsilon(|\mathbf{E}(x', y', z')|) - \varepsilon^{ext}.$$

Let's assume $\mathbf{E}^{ext}(x, y, z) = E_0\mathbf{E}_1^{exy}(x, y, z)$, where $\mathbf{E}_1^{ext}(x', y', z')$ field of a single amplitude; $\mathbf{E}(x', y', z') = E_0\mathbf{E}_1^{exy}(x', y', z')$. We obtain

$$\mathbf{E}_1(x, y, z) = \mathbf{E}_1^{ext}(x, y, z) + [\text{grad div} + k^2] \times \int_V G(\overline{x}, \overline{y}, z, z')\tau\,\mathbf{E}_1(x', y', z')dv',$$

$$x, y, z \in V \tag{10}$$

Let's introduce the function $\mathbf{D} = \tau\mathbf{E}_1$ and transform (10):

$$\frac{\mathbf{D}(x, y, z)}{\tau(x, y, z)} = \mathbf{E}_1^{ext}(x, y, z) + [\text{grad div} + k^2] \times \int_V G(\overline{x}, \overline{y}, z, z')\mathbf{D}(x', y', z')dv',$$

$$x, y, z \in V \tag{11}$$

where

$$\tau(|\mathbf{E}(x', y', z')|) = \varepsilon\left(\left|E_0\,\frac{1}{\tau}\,\mathbf{D}(x', y', z')\right|\right) - \varepsilon^{ext}. \tag{12}$$

Equation (11) is solved by successive approximations $E_0^{(p)} = E_0\,\frac{p}{P}$, $p = 1, \ldots P$, $E_0^{(0)}$ — linear approximation,

$$\frac{\mathbf{D}^{(p)}(x, y, z)}{\tau^{(p)}(x, y, z)} = \mathbf{E}_1^{ext}(x, y, z) + [\text{grad div} + k^2] \times \int_V G(\overline{x}, \overline{y}, z, z')\mathbf{D}^{(p)}(x', y', z')dv',$$

$$x, y, z \in V \tag{13}$$

where $\tau^{(p)}(x, y, z)$ is defined from (12), where $\mathbf{D}(x', y', z') = \mathbf{D}^{(p-1)}(x', y', z')$.

Perturbation method — first step of iteration method. In (12) $\mathbf{D}(x', y', z')$ — solution of a linear IDE, $\tau$ — inhomogeneous inside an object and also depends on linear solution.

For dielectric bodies on a layered dielectric substrate, the Green's function his of tensor nature [23]. However, the IDE transformations are the same.

It should be noted that the nonlinear part is located on the left side of equation (13), therefore, the solution method (13) and the program for a linear dielectric can easily be transformed into a method and program for a nonlinear dielectric. Compared to the linear approximation, only diagonal elements due to the first (free) term in (13) are changing.

IDEs (13) with respect to an unknown linear function were solved by the Galerkin method, similar to how it is done in [23,24]:

$$\mathbf{D}^{(p)}(x', y', z') = \sum_m \mathbf{X}_m^{(p)}V_m(x', y', z'),$$

where $\mathbf{X}_m^{(p)}$ is a matrix of unknown coefficients, $V_m(x', y', z')$ scalar basis functions independent of the step number of the iterative process. As a result, by using Galerkin method we'll obtain SLAE relative to $\mathbf{X}_m^{(p)}$. Moreover, SLAE matrix elements generated by the integro-differential term in (13) are the same as when solving a similar linear problem. They do not depend on the step number of the iterative process. Unlike the linear problem, SLAE matrix elements generated by the free term (13) are found by numerical integration.

After solving SLAE we find the diffracted field, which is defined by (13) at $x, y, z \notin V$

## 4. Numerical results

Figure 1 shows the results of calculating the reflection of a Gaussian pulse with a duration of $\tau = 0.1$ ns, with a carrier frequency of 1 THz. Parameters of dielectric layer — $\varepsilon = 2$, $h = 26.5\,\mu$m, substrate $\varepsilon_s = 4$. Parameters of graphene $\mu_c = 0.25$ eV, temperature 300 K, relaxation time 1 ps. The incidence is normal. $R_{1,3}$ — first and third harmonics power reflectance coefficients. The electric field strength during graphene breakdown is more than 1.2 MV/cm [25].

Calculation method — the spectrum of the incident pulse was found, then the spectrum of the reflected and transmitted pulses was calculated according to the described method, after numerical inverse Fourier transformation these pulses were found. Since the conductivity of graphene depends on the square of the amplitude of the electric field strength, the amplitudes of reflected pulses at both the main and third harmonics are not directly proportional to the amplitude of the incident pulse.

As in [16], the error of the perturbation method for this structure is several percents (less than 5). Maximum error at frequencies less than 1 THz. This is due to the fact that the conductivity of graphene ($\sigma_1$ and $\sigma_3$) increases with the drop of frequency. The discrepancy is not fundamental, but it should be taken into account when calculating nonlinear graphene structures in the field of plasmon resonance.

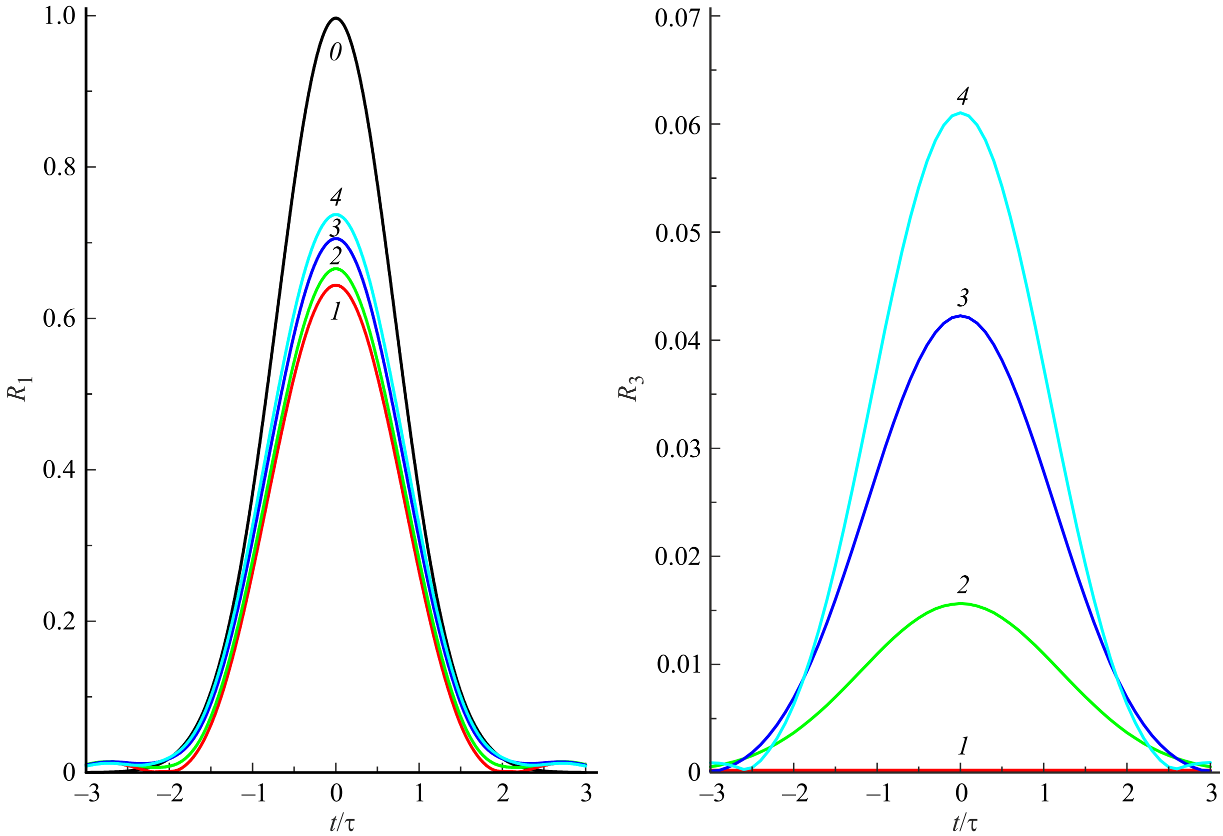


**Figure 1.** Reflection of a Gaussian pulse from a graphene layer. Curve *0* — incident pulse (normalized to maximum), curves *1* — linear mode, *2* — electrical field strength in the maximum of incident pulse $E_0 = 3$ MV/cm, *3* — $E_0 = 5$ MV/cm, *4* — $E_0 = 9$ MV/cm.

Figure 2 shows the dependences of reflection coefficients on a nonlinear layer at various dimensionless normalized external field strengths $U_0 = E_0\sqrt{\alpha}$. The wavelength is normalized to the layer thickness $h$. Parameters $\varepsilon_{lin} = 9$, dielectric permittivity of the substrate 2.25. It can be seen from Fig. 2 that the effect of self-action is mainly manifested near the minimum of the reflectance coefficient $R_1$.

Comparison of the perturbation method (number of iterations $P = 2$) and the iterative method is shown in Fig. 3. Parameters of the structure are the same as in Figure 2: The main discrepancy is observed at high field strengths and short wavelengths. When comparing, it should be taken into account that both the iterative method and the perturbation method have the same number of layers $N$ into which the nonlinear layer was divided.

Now let's consider diffraction on the non-linear dielectric strip grating. Figure 4 shows the unit cell of such a diffraction grating (DG), a shaded rectangle — a cross-section of a nonlinear dielectric strip. The grating is infinite in the direction perpendicular to the plane of the drawing. The figure shows a single-layer substrate, but the number of layers in the program is arbitrary. Up to 100 layers were tested. The method is described in [23] and in other papers, the main difference, as mentioned above, is numerical, and not analytical (as in the case of linear problem) integration when calculating matrix elements due to the free term in (13).

One of the method and program tests is transition from the DG to the continuous layer at. The results are presented in Fig. 2 as asterisks.

Some results of calculation of non-linear DGs are given in Fig. 5, 6. The width of the dielectric strips $L = d/2$, thickness $h = d$, linear part of the dielectric permittivity $\varepsilon_{lin} = 9$, dielectric permittivity of the substrate 2.25; $s$-polarization —vector **E** is perpendicular the plane of incidence along the dielectric strips, magnetic field in the plane of incidence; $p$-polarization — vector **H** is perpendicular to the plane of incidence. At $p$-polarization — transverse resonance is observed — reflectance is close to unity (Fig. 5). Even a small non-linearity leads to a significant change in characteristics. This is especially noticeable near the resonance.

The error of perturbation method (Fig. 6) is several percent, with the exception of short wavelengths with $s$ polarization.

## Conclusions

Analytical and numerical-analytical methods have been developed for solving nonlinear boundary value problems

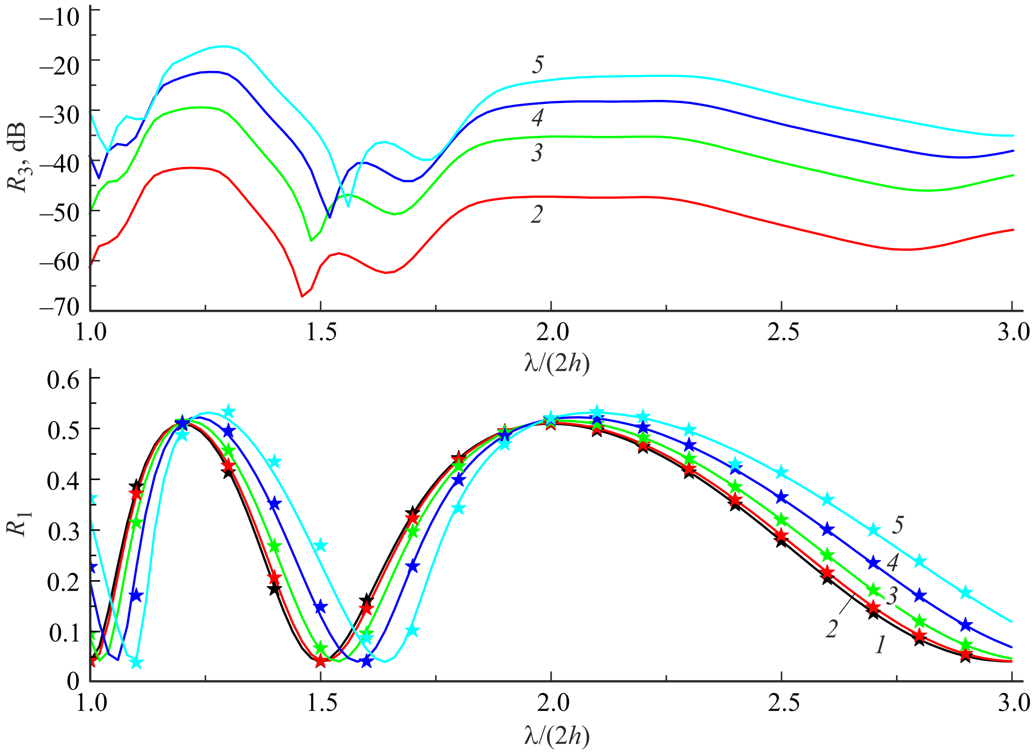


**Figure 2.** Reflection from the non-linear layer. The incidence is normal. $R_p$ — power reflectance coefficient. Curve *1* — $U_0 \ll 1$, *2* — $U_0 = 0.5$, *3* — $U_0 = 1$, *4* — $U_0 = 1.5$, *5* — $U_0 = 2$. Asterisks — calculation in the program for nonlinear diffraction grating.

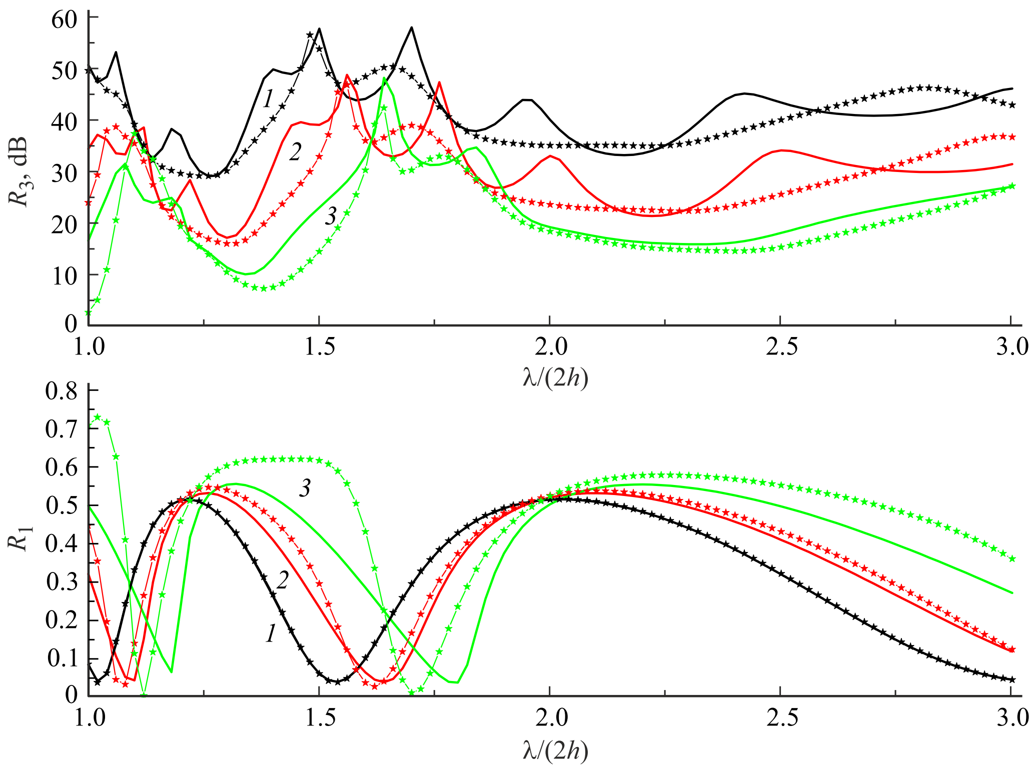


**Figure 3.** Comparison of the calculation results obtained by iterative method (solid curves) and perturbation method (curves with asterisks). Digits of curves — normalized strength of external field.

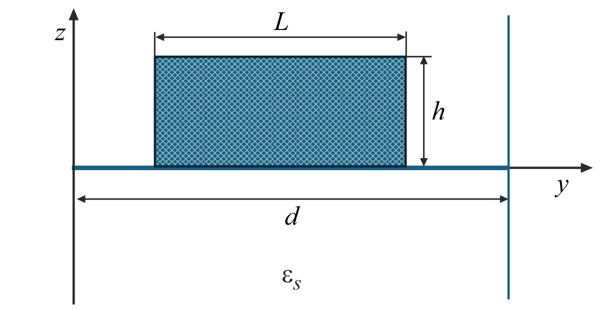


**Figure 4.** Unit cell of diffraction grating.

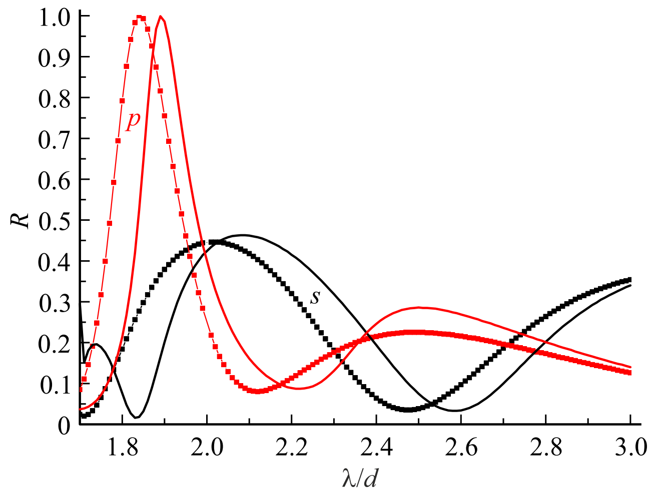


**Figure 5.** Reflectance of the main spatial harmonic with nonlinear dielectric strips versus normalized wavelength. Self-action. $U_0 = 1$. Characters $p, s$ denote $p$- and $s$-polarization of the incident wave. Curves without symbols — iteration method, with symbols — linear approximation.

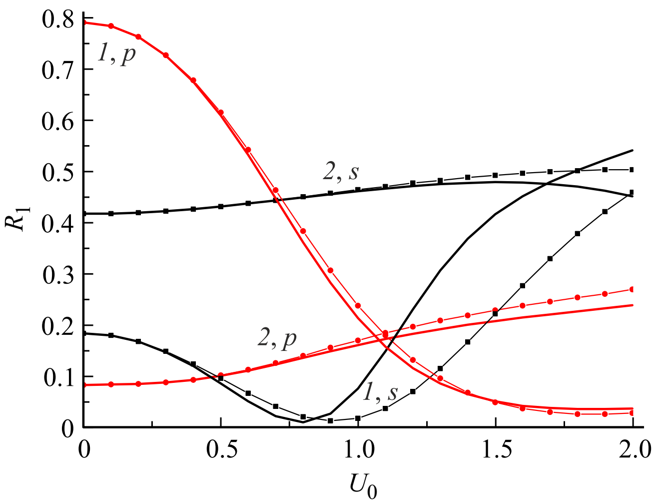


**Figure 6.** Reflectance of the main spatial harmonic with nonlinear dielectric strips versus normalized strength of electrical field under normally incident plane wave on the diffraction grating. Self-action. $1 — \lambda/d = 1.8$, $2 — \lambda/d = 2.1$. Characters $p, s$ standing after the curve number denote $p$- and $s$-polarization of the incident wave. Curves without symbols — iteration method, with symbols — linear approximation.

of electromagnetic wave reflection from a graphene layer and a dielectric layer, problems of diffraction on a dielectric body. It was demonstrated that non-linear IDE may be transformed to IDE with a linear integral term and a non-linear free term. This greatly increases the calculations rate. Computer programs in C language have been developed for numerical modeling of these objects. The perturbation method error was tested.

## Funding

This study was supported financially by the Ministry of Science and Higher Education of the Russian Federation (State Assignment in the field of scientific activity № FENW-2022-0001).

## Conflict of interest

The authors declare that they have no conflict of interest.

## References

[1] J. Wang, S.A. Maier, A. Tittl. Adv. Opt. Mater., **10** (7), 2102366 (2022).
[2] A.S. Solntsev, G.S. Agarwal, Y.S. Kivshar. Nat. Photonics, **15**, 327 (2021).
[3] M.J. Huttunen, S. Bin-Alam, O. Reshef, Y. Mamchur, T. Stolt, J.-M. Menard, K. Dolgaleva, R.W. Boyd, M. Kauranen. 2020 22nd Int. Conf. on Transparent Optical Networks (ICTON). DOI: 10.1109/ICTON51198.2020.9203026
[4] T. Santiago-Cruz, S.D. Gennaro, O. Mitrofanov, S. Addamane, J. Reno, I. Brener, M.V. Chekhova. Science, **377**, 991(2022).
[5] M.J. Huttunen, R. Czaplicki, M. Kauranen. J. Nonlinear Opt. Phys. Mater., **28**, 1950001 (2019).
[6] D. Hähnel, C. Golla, M. Albert, T. Zentgraf, V. Myroshnychenko, J. Förstner, C. Meier. Light Sci. Appl., **12**, 97 (2023). https://doi.org/10.1038/s41377-023-01134-1
[7] Hui-Hsin Hsiao, Jou-Chun Hsieh, Ai-Yin Liu, Kuang-I Lin, Yi-Chien Hsu. Nanophotonics, **13** (17), (2024). DOI: org/10.1515/nanoph-2024-0194
[8] Y. Ra'di, N. Nefedkin, P. Popovski, A. Alù. IEEE Antennas and Propagation Magazine, **66** (5), 52 (2024).
[9] J. Noh, T. Santiago-Cruz, S.D. Gennaro. V. Sultanov, I. Brener, M.V. Chekhova. CLEO Optica Publishing Group, FM3O.1 (2024).
[10] J.H. Krakofsky, S. Stich, G. Böohm, M.A. Belkin. CLEO Optica Publishing Group, SM4P.3. (2024).
[11] M.D. Feinstein1, A. Adronikides, E. Almeida. CLEO Optica Publishing Group, FTh1P.6. (2024).
[12] I. Brener. 2024 Intern. Conf. on Optical MEMS and Nanophotonics (OMN). DOI: 10.1109/OMN61224.2024.10685263
[13] S.A. Mikhailov. Europhys. Lett., **79**, 27002 (2007).
[14] E. Hendry, P.J. Hale, J. Moger, A.K. Savchenko, S.A. Mikhailov. Phys. Rev. Lett., **105**, 097401 (2010).
[15] V.V. Cherepanov. *Electrodinamicheskiy analis plasmonnykh ustroistv na osnove grafena v TGz i IK diapazone* (Avtoref. kand. diss. YuF, Rostov-on-Don, 2023) (in Russian).
[16] A.M. Lerer. J. Commun. Technol. Electron., **57** (11), 1151 (2012). DOI: 10.1134/S106422691210004X
[17] G.W. Hanson. J. Appl. Phys., **103** (6), 064302 (2008).

[18] J.L. Cheng, N. Vermeulen, J. Sipe. Phys. Rev. B, **91**, 235320 (2015).
[19] S.A. Mikhailov. Phys. Rev. B, **93** (8), 085403 (2016).
[20] V.V. Cherepanov. Physicheskie osnovy pryborostroeniya **9** (4), 2 (2020) (in Russian).
[21] G.A. Kalinchenko, A. Lerer. J. Electromagnetic Waves and Application, **13** (11), 1539 (1999).
[22] A.M. Lerer, I.N. Ivanova. Tr. conf. *Analyticheskiye i chislenniye metody modelyrovania estestvenno-nauchnykh i sotsialnykh problem AChM-2023*. Set of articles on materials of the XVIII all-Russian conference ANM-2023 with the participation of foreign organizations. (Pensa, Russia, 2023), v. 1. v. 44.
[23] A.M. Lerer. J. Commun. Technol. Electron., **57** (11), 1151 (2012). DOI: 10.1134/S106422691210004X
[24] A.M. Lerer, G.S. Makeeva, V.V. Cherepanov. J. Commun. Technol. Electron., **66** (6), 656 (2021). DOI: 10.1134/S1064226921060188
[25] M.E. Abbassi, L. Pósa, P. Makk, C. Nef, K. Thodkar, A. Halbritter., M. Calame. Nanoscale, **9**, 17312 (2017). DOI: 10.1039/C7NR05348G

*Translated by T.Zorina*